The EMBO Journal (2012) 31, 3239–3251 | © 2012 European Molecular Biology Organization | All Rights Reserved 0261-4189/12
www.embojournal.org

THE EMBO JOURNAL

Impairment of GABAB receptor dimer by endogenous 14-3-3ζ in chronic pain conditions

Sophie Laffray[1,2], Rabia Bouali-Benazzouz[1,2,7], Marie-Amélie Papon[1,2,7], Alexandre Favereaux[1,2], Yang Jiang[3], Tina Holm[3], Corentin Spriet[4], Pascal Desbarats[5], Pascal Fossat[1,2], Yves Le Feuvre[1,2], Marion Decossas[6], Laurent Héliot[4], Ulo Langel[3], Frédéric Nagy[1,2] and Marc Landry[1,2,*]

[1]Bordeaux University, Bordeaux, France, [2]IINS, CNRS UMR 5297, Bordeaux, France, [3]Department of Neurochemistry, Stockholm University, Stockholm, Sweden, [4]Laboratoire d'Imagerie Cellulaire Fonctionnelle, Institut de Recherche Interdisciplinaire, Lille, France, [5]LaBRi, CNRS UMR 5800, Bordeaux University, Bordeaux, France and [6]Bordeaux Imaging Center, Bordeaux University, Bordeaux, France

In the central nervous system, the inhibitory GABAB receptor is the archetype of heterodimeric G protein-coupled receptors (GPCRs). However, the regulation of GABAB dimerization, and more generally of GPCR oligomerization, remains largely unknown. We propose a novel mechanism for inhibition of GPCR activity through de-dimerization in pathological conditions. We show here that 14-3-3ζ, a GABAB1-binding protein, dissociates the GABAB heterodimer, resulting in the impairment of GABAB signalling in spinal neurons. In the dorsal spinal cord of neuropathic rats, 14-3-3ζ is overexpressed and weakens GABAB inhibition. Using anti-14-3-3ζ siRNA or competing peptides disrupts 14-3-3ζ/GABAB1 interaction and restores functional GABAB heterodimers in the dorsal horn. Importantly, both strategies greatly enhance the anti-nociceptive effect of intrathecal Baclofen in neuropathic rats. Taken together, our data provide the first example of endogenous regulation of a GPCR oligomeric state and demonstrate its functional impact on the pathophysiological process of neuropathic pain sensitization.

The EMBO Journal (2012) **31,** 3239–3251. doi:10.1038/emboj.2012.161; Published online 12 June 2012
Subject Categories: signal transduction; neuroscience
Keywords: disinhibition; G protein-coupled receptor; neuropathic pain; oligomer; spinal cord

Introduction

G protein-coupled receptors (GPCRs) modulate a wide range of physiological processes and new drug candidates are continually being developed for selective GPCRs (Lagerstrom and Schioth, 2008; Panetta and Greenwood, 2008). Evidence indicate that a large variety of GPCRs exist as oligomers (Bouvier, 2001; Szidonya *et al*, 2008), and that GPCR function is highly dependent on their oligomeric state (Gurevich and Gurevich, 2008). Furthermore, changes in GPCR oligomerization are involved in pathophysiological conditions such as psychosis (Gonzalez-Maeso *et al*, 2008). Functional GABAB receptors are prototypical of dimeric class C GPCRs, expressed as obligate heterodimers of the two subunits GABAB1 (B1) and GABAB2 (B2) (Jones *et al*, 1998; Kaupmann *et al*, 1998). In addition, core GABAB dimers can also form higher order multimers in association with themselves (Comps-Agrar *et al*, 2011), or with auxiliary subunits (Schwenk *et al*, 2010). Because GABAB inhibitory activity strictly depends on its dimeric state (Bowery, 2006), it may be postulated that altered GABAB dimerization has pathophysiological implications. Actually, aalthough the GABAB agonist Baclofen has anti-nociceptive properties (Malcangio and Bowery, 1996; Schuler *et al*, 2001; Bowery *et al*, 2002), its effectiveness is limited in clinic (Loubser and Akman, 1996) or in rat pain models (Franek *et al*, 2004; Wang *et al*, 2007). But the limitation of Baclofen effects does not rely on classical desensitization through ligand-induced endocytosis since internalized GABAB receptors are constitutively sorted to recycling endosomes for rapid reinsertion into the plasma membrane (Perroy *et al*, 2003; Fairfax *et al*, 2004; Laffray *et al*, 2007; Grampp *et al*, 2008; Vargas *et al*, 2008).

In this context, we demonstrate a novel alternative mechanism accounting for GABAB dysfunction based on the impairment of GABAB subunit association, triggered by 14-3-3ζ, a B1-interacting protein (Couve *et al*, 2001). Moreover, we provide evidence for the involvement of such a 14-3-3ζ-induced GABAB de-dimerization in spinal sensitization to neuropathic pain. We show that 14-3-3ζ is overexpressed in the dorsal horn of neuropathic rats and impedes GABAB inhibition. We further show that GABAB efficiency can be rescued by *in-vivo* application of either anti-14-3-3ζ siRNA, or cell-penetrating peptides that reverse B1/14-3-3ζ interaction.

Taken together, our findings demonstrate that regulating the oligomeric state represents a novel process to modulate GPCR activity, and is an endogenous mechanism occurring *in vivo* in pathophysiological conditions. We show that GABAB dissociation can be targeted to limit central sensitization to pain, suggesting new therapeutical approaches.

Results

14-3-3ζ expression is increased in the spinal dorsal horn of neuropathic rats

Since GABAB is involved in the modulation of nociceptive transmission (Bowery, 2006), we first studied 14-3-3ζ expression in rats with spinal nerve ligation (SNL), i.e., rats with neuropathic behaviour. With *in-situ* hybridization, a marked increase was observed in the intensity of 14-3-3ζ

*Corresponding author. IINS, CNRS UMR 5297, Bordeaux Segalen University, Université Bordeaux 2, 146 rue Leo-Saignat, Bordeaux 33077, France. Tel.: +33 5 57 57 40 50; Fax: +33 5 57 57 40 51; E-mail: marc.landry@u-bordeaux2.fr
[7]These authors contributed equally to this work

Received: 10 November 2011; accepted: 7 May 2012; published online: 12 June 2012

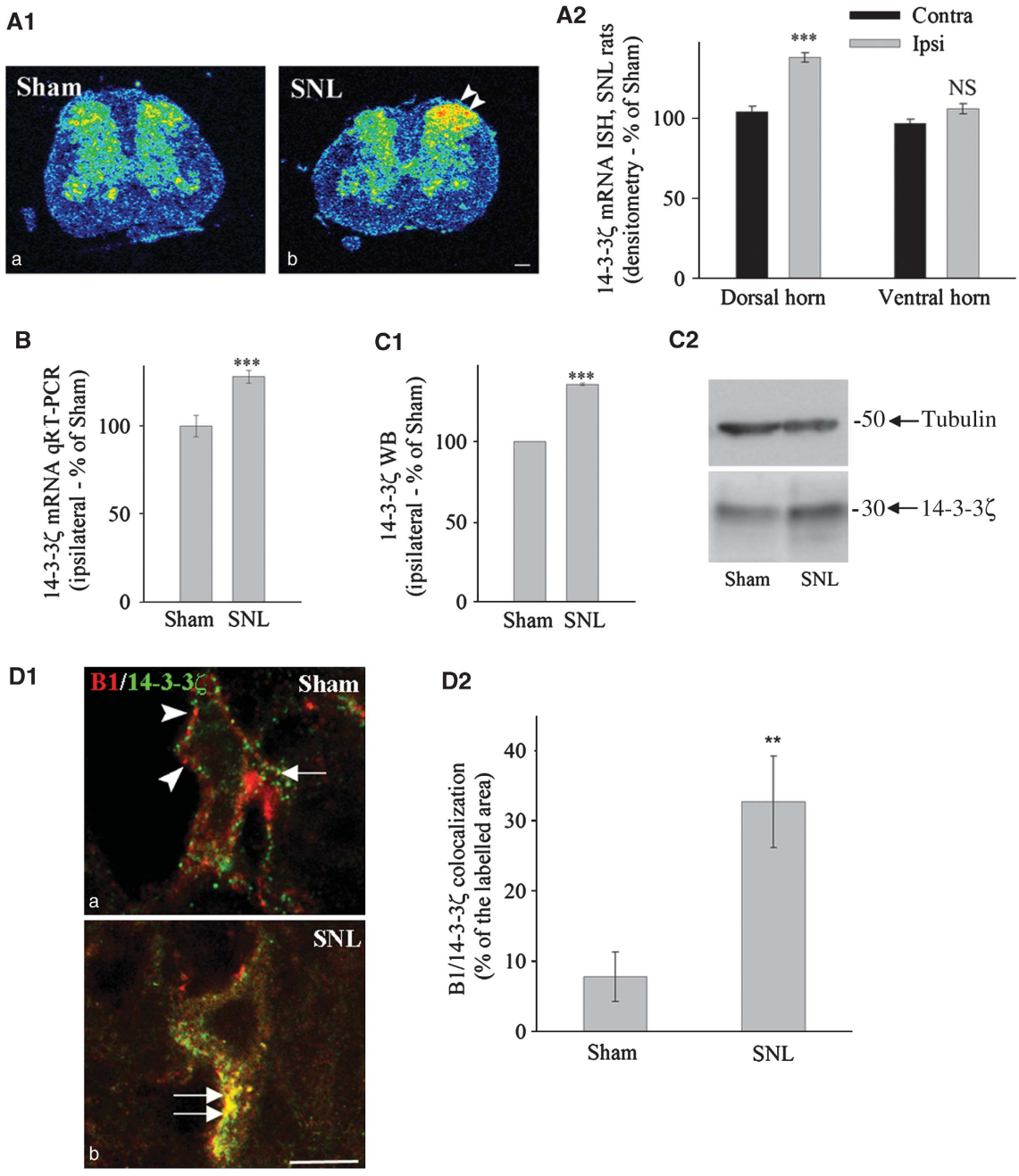

Figure 1 Increased expression of 14-3-3ζ in the spinal cord of neuropathic rats. (**A1**) *In-situ* hybridization to 14-3-3ζ mRNA illustrated with autoradiographic films showing an increase in ipsilateral dorsal horn of SNL rats (double arrowhead in (b)). Bar: 200 μm. (**A2**) Quantification of *in-situ* hybridization by densitometry ($n = 5$ in each group). (**B**) qRT–PCR measurement of 14-3-3ζ mRNA ($n = 5$ in each group). (**C1**) Mean intensity of 14-3-3ζ immunoblot. (**C2**) Example of 14-3-3ζ immunoblot. (**B**, **C1**) % ± s.e.m. of the reference value (sham) set to 100%, $n = 5$ in each condition. (**D1**) Double immunohistochemistry for B1 (arrowheads in (a)) and 14-3-3ζ (arrow in (a)) in spinal cord sections of sham (a) and SNL (b) rats. B1 subunit and 14-3-3ζ colocalization is enhanced after nerve injury (b, double arrow). (**D2**). Quantification of colocalization between GABAB1 and 14-3-3ζ ($n = 4$ rats in each group). $^{***}P < 0.001$; $^{**}P < 0.01$; NS = non-significant; Contra = Contralateral; Ipsi = Ipsilateral to the nerve ligation.

mRNA labelling in the ipsilateral dorsal but not in ventral horn of SNL rats (Figure 1A1; Supplementary Figure S1A1). Quantification by densitometry and grain counting confirmed this increased expression (Figure 1A2; Supplementary Figure S1A2) that was further assessed with qRT–PCR (Figure 1B). Upregulation was not found in dorsal root ganglia, or for 14-3-3η mRNA, the other isoform possibly interacting with B1 (Couve *et al*, 2001; (Supplementary Figure S1B–E; Supplementary data). Expression of 14-3-3ζ protein was examined by western blotting in total extracts of ipsilateral lumbar spinal cord. The quantification showed an increase of protein level in the ipsilateral spinal cord of SNL animals (Figure 1C1, $P < 0.001$; Figure 1C2). GABAB subunits and 14-3-3ζ were found in most neuronal cell bodies of the spinal cord; however, subcellular colocalization between B1 and 14-3-3ζ was increased in SNL as compared with sham animals (Figure 1D1 and D2). 14-3-3ζ was not found in presynaptic nerve endings from primary afferents or local

interneurons in Sham rats while it is located in postsynaptic compartments (Supplementary Figure S2A, left panel). In contrast, when overexpressed in SNL rats, 14-3-3ζ is seen in both presynaptic and postsynaptic compartments (Supplementary Figure S2A, right panel), indicating possible interactions with both GABAB1a (pre-) and GABAB1b (post-) subtypes of the GABAB1 subunit (Vigot *et al*, 2006). Taken together, our results showed that (i) 14-3-3ζ was specifically overexpressed in dorsal horn neurons in neuropathic pain conditions and (ii) 14-3-3ζ was colocalized with GABAB1 in spinal neurons of SNL rats.

B1 interaction with 14-3-3ζ impairs GABAB subunits association in cultured neurons

We used cultured spinal neurons to investigate cellular interactions between tagged recombinant 14-3-3ζ and GABAB subunits (Flag–14-3-3ζ, myc–B1b and HA–B2). When B1b and B2 were co-expressed, the immunostaining for both was largely overlapping (Figure 2Aa–c). In contrast, the expression of 14-3-3ζ induced the loss of B2 staining in subcellular domains where 14-3-3ζ was expressed (Figure 2Ad–g). The colocalization between B1b and B2 decreased from 58 ± 4% in double transfected cells to 17 ± 3.1% in triple transfected cells (Figure 2B; $P<0.01$). The quantification also showed that 14-3-3ζ was preferentially colocalized with B1b, rather than with B2 (Figure 2B; $P<0.05$). In addition, we demonstrated that similar changes occur in the colocalization of endogenous B1 and B2 upon Flag–14-3-3ζ overexpression in cultured spinal neurons (Supplementary Figure S3A1–A3).

Next, we addressed whether these colocalized proteins belong to the same complex. Therefore, we developed a method to analyse in parallel the colocalization and correlation of staining intensities (see Supplementary data). In double transfected cells, variations in labelling intensities for B1b and B2 appeared strongly correlated as expected for heterodimers (Figure 2C; +0.64). In triple transfected cells, only labelling intensities for B1b and 14-3-3ζ were positively correlated indicating their association (Figure 2C; +0.46). In contrast, B1b and B2 staining intensities varied randomly, although the two subunits remained partially colocalized (Figure 2C; −0.13). In summary, 14-3-3ζ overexpression resulted in a decreased colocalization and correlation between B1b and B2, but an increased correlation between B1b and 14-3-3ζ.

Then, we confirmed the interaction between B1b and 14-3-3ζ that was originally demonstrated by Couve *et al* (2001) (Supplementary Figure S3B–D; Supplementary data). Subsequently, we used biochemical (co-immunoprecipitation, co-IP) and biophysical (two-photon fluorescence lifetime imaging measurement, 2P-FLIM) methods to test possible dissociation of the GABAB heterodimer by 14-3-3ζ. (i) COS cells were transfected with myc–B1b and HA–B2, with or without Flag–14-3-3ζ (Figure 2D). As expected, we found co-IP of B2 and B1b in the absence of 14-3-3ζ (left panel). In contrast, when 14-3-3ζ was also expressed, B2 did not co-precipitate with B1b (right panel), and was detected in the supernatant only at low levels. Inhibition of lysosomal activity increases the amount of B2 in protein extracts from COS cells after 14-3-3ζ overexpression (Supplementary Figure S3E). This indicates that B2 subunit is trafficked towards the lysosomes for degradation after 14-3-3ζ-induced heterodimer dissociation. The loss of B2 subunit at the membrane where 14-3-3/B1 complexes are formed is consistent with the decreased stability of B2 alone at the membrane in cultured cells (Galvez *et al*, 2001). Since the ASA mutation does not impede GABAB heterodimerization (Brock *et al*, 2005) but inhibits the interaction between B1 and 14-3-3ζ (Supplementary Figure S3D), we used the $B1_{ASA}$ mutant as a negative control of 14-3-3ζ-induced effects (Figure 2E). We showed that B2 remained associated with $B1_{ASA}$ in the presence of 14-3-3ζ (right panel), indicating that the heterodimer was not disrupted when 14-3-3 protein was unable to bind a mutant B1 subunit. (ii) In neuronal cultures, we used 2P-FLIM to calculate Fluorescence or Förster Resonance Energy Transfer (FRET) efficiency between GFP-B1b and t-dimer DsRed-B2 (Figure 2F). The co-expression of B1b and B2 triggers FRET interactions with a mean efficiency of around 20%, showing their association in a heterodimer (Figure 2F, 'B1b/B2'). Expression of 14-3-3ζ induced a decrease in FRET efficiency by >50% (Figure 2F, 'B1b/B2/14-3-3ζ' versus 'B1b/B2'; $P<0.05$). The same effect of 14-3-3ζ was noticed on heterodimers made of the GABAB1a splice variant (Supplementary Figure S3F). To ensure the specificity of 14-3-3ζ-induced dissociation of the heterodimer, we developed an anti-14-3-3ζ siRNA strategy (Supplementary Figure S4; Supplementary data). We incubated triple transfected cells with this anti-14-3-3ζ siRNA (Figure 2F, 'B1b/B2/14–3–3ζ/siRNA'). FRET efficiency was not significantly different from double transfected cells ('B1b/B2'), indicating that 14-3-3ζ effects were suppressed. In contrast, control RNA (mismatch, mmRNA) did not modify 14-3-3ζ-induced inhibition of B1b/B2 interaction (Figure 2F, 'B1b/B2/14-3-3ζ/mmRNA').

Since siRNA knocks down all 14-3-3 proteins, they may induce unwanted side effects. For this reason, we also developed 14-3-3ζ competing peptides as short peptidergic analogues of the B1 C-terminus (Supplementary Figures S5 and S6; Supplementary data). As compared with siRNA, competing peptides mimic only a subclass of binding partners among >300 possible (Pozuelo Rubio *et al*, 2004), which confers higher selectivity to the peptides. Thus, we investigated with 2P-FLIM the role of these peptides to inhibit 14-3-3ζ-induced changes in GABAB dimeric state. Co-transfection with 14-3-3ζ induced significant decrease in FRET interactions between B1b and B2 (Figure 2G; 'B1b/B2/14-3-3ζ' versus 'B1b/B2'; $P<0.05$). Incubation of triple transfected neurons with pVEC-B1 (922–930) restored a similar FRET efficiency to that observed in double transfected cells (Figure 2G; '+ pVEC-B1 (922–930)' versus 'B1b/B2/14-3-3ζ'; $P<0.05$).

The transfection of 14-3-3η, another member of the 14-3-3 family, was used as a control. It showed no change in B1 and B2 interaction (Supplementary Figure S7A and B), demonstrating the specificity of 14-3-3ζ effects.

Then, we explored the subcellular compartment where GABAB dissociation occurred. We measured the effect of 14-3-3ζ overexpression on FRET efficiency in three distinct regions of interest delineated with appropriate markers (see Supplementary data), i.e., the endoplasmic reticulum, Golgi Apparatus and plasma membrane (Figure 3A1). Decrease of FRET efficiency was detectable at the plasma membrane, but not in the endoplasmic reticulum or Golgi (Figure 3A2), suggesting that de-dimerization affects only GABAB heterodimers already inserted at the plasma membrane. Surprisingly, FRET efficiency was even increased in the endoplasmic reticulum, probably due to indirect effects

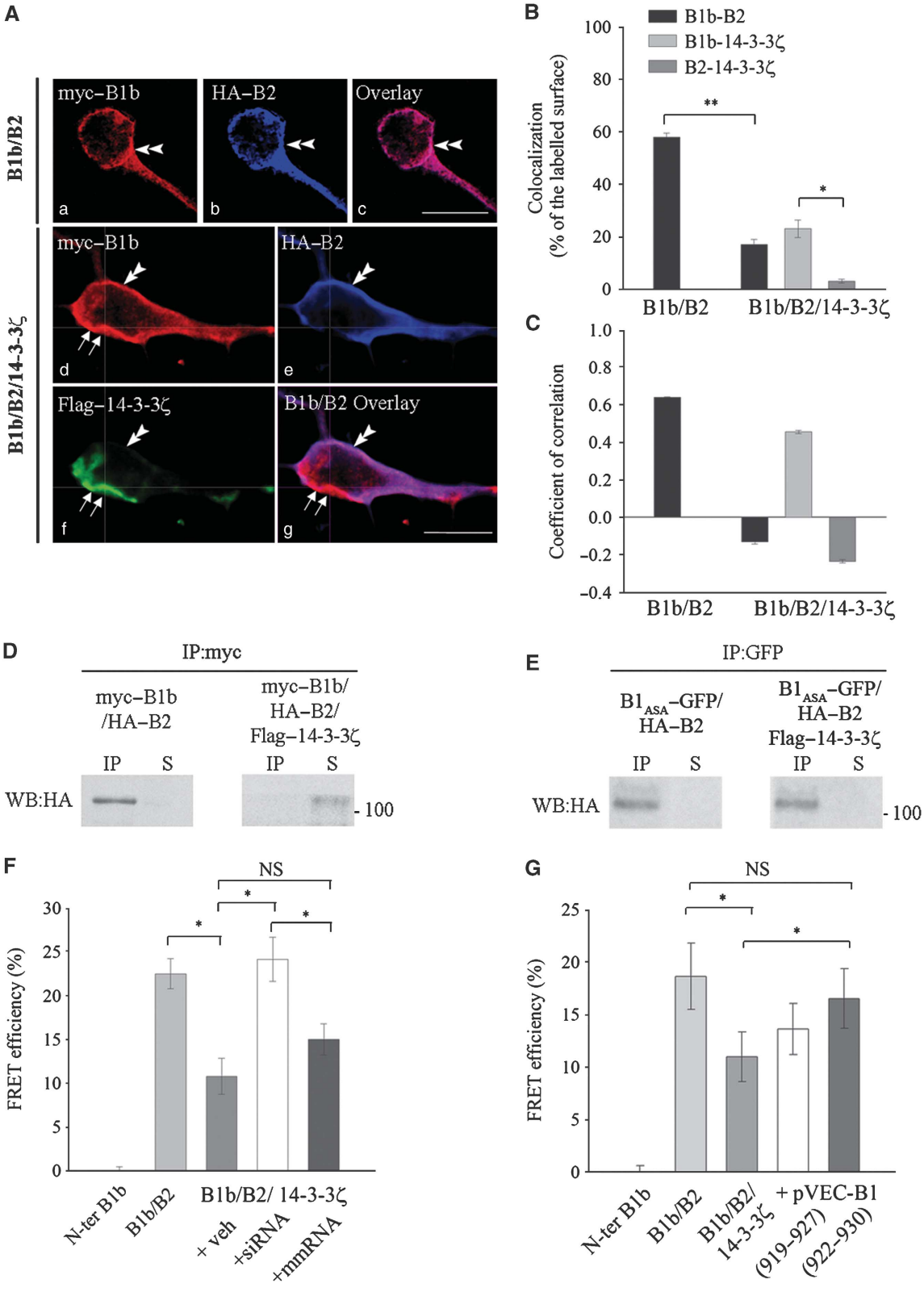

of 14-3-3ζ overexpression. An additional experiment was performed according to a protocol of double immunoprecipitation derived from Holman and Henley (2007). COS cells were first transfected with B1b and B2, and either GFP or 14-3-3ζ. They were then treated with sulfo-NHS-SS-biotin for surface biotinylation. After lysis, total cell extracts were incubated with an anti-myc antibody and the GABAB complexes were pull down with Protein G Sepharose beads. Membrane fraction was then retrieved by a second immunoprecipitation with Streptavidin Agarose beads.

Figure 2 14-3-3ζ dissociation of the GABAB heterodimer in cultured spinal neurons. (**A**) (a–c) Double transfected cells (B1b/B2) showing myc–B1b (a, red) and HA–B2 (b, blue) colocalization at the plasma membrane (double arrowheads). Bar: 20 μm. (d–g) Triple transfected cells (B1b/B2/14-3-3ζ) showing that B1b (d, red) and 14-3-3ζ (f, green) colocalize in domains lacking B2 (double arrows) while B1b and B2 (e, blue) remain colocalized in the absence of 14-3-3ζ (double arrowhead). Bar: 10 μm. (**B**) Colocalization in double (B1b/B2; $n=18$) and triple (B1b/B2/14-3-3ζ; $n=16$) transfected neurons. $^{*}P<0.05$; $^{**}P<0.01$. (**C**) Correlation of labelling intensity in double (B1b/B2; $n=18$) and triple (B1b/B2/14-3-3ζ; $n=16$) transfected neurons. (**D**) In double transfected COS-7 cells, HA–B2 co-precipitates with myc–B1b (left panel). In triple transfected cells, the interaction between B1 and B2 subunits is abolished (right panel) ($n=3$ independent experiments). (**E**) In double and triple transfected cells, HA–B2 co-precipitates with $B1_{ASA}$-GFP that does not interact with 14-3-3ζ (see Supplementary Figure S3B and C) ($n=3$ independent experiments). IP lanes: co-IP; S lanes: supernatant. (**F**, **G**) FRET efficiency (mean % ± s.e.m., $n=31$ or 21 cells) between N-ter GFP (B1b), and t-dimer DsRed (B2) in primary cultures transfected with GFP-B1b and t-dimer DsRed-B2 alone (B1b/B2), or together with Flag–14-3-3ζ (B1b/B2/14-3-3ζ). Cultures are further incubated with iFect (veh), anti-14-3-3 siRNA (+siRNA), or mismatch RNA (+mmRNA) (**F**) or competing peptides (+pVec-B1 919–927 or 922–930) (**G**). $^{*}P<0.05$. NS = non-significant.

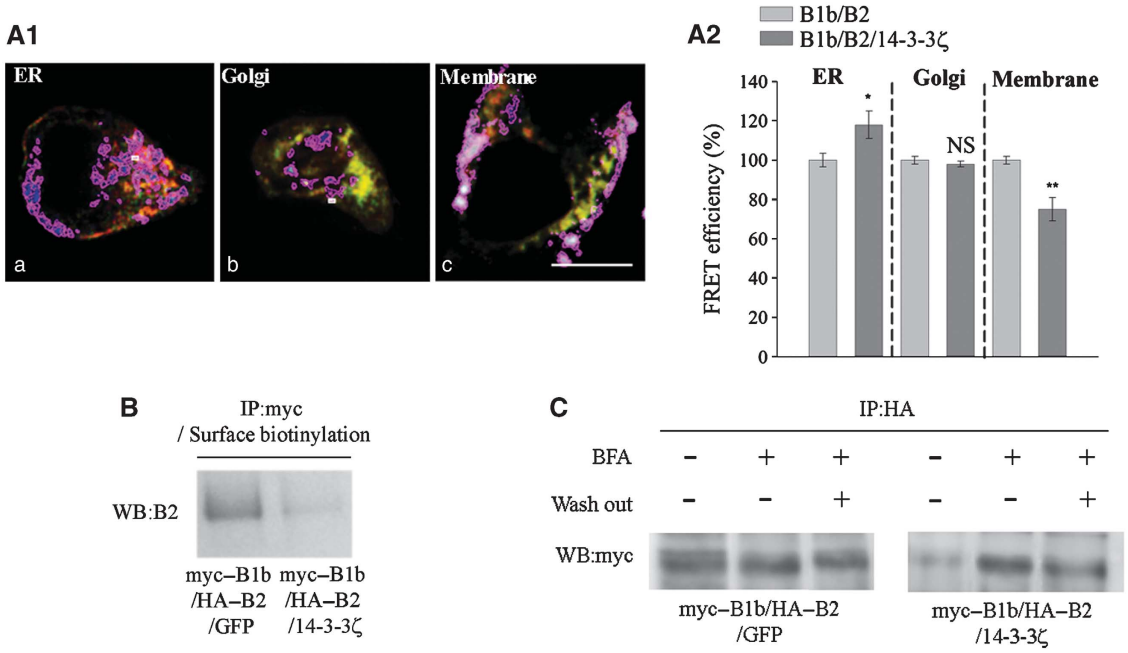

Figure 3 Dissociation of the GABAB heterodimer at the plasma membrane. (**A1**) FRET analysis in regions of interest identified with a mask (delineated with a purple line) drawn over areas positive for anti-calreticulin (a, ER marker), anti-mannosidase II (b, Golgi marker) or DiD (c, lipophilic carbocyanine used as a marker for the plasma membrane). (**A2**) FRET efficiency between GFP–B1b and t-dimer DsRed-B2 is decreased at the plasma membrane (right). No changes are found in the Golgi, and an increase in FRET efficiency is even detected in the ER ($n=15$ cells in each conditions). (**B**) COS-7 cells were transfected and processed for double immunoprecipitation. The surface fraction of the GABAB complexes was then isolated and probed on western blot with an anti-B2 antibody. The association between B2 and B1 at the plasma membrane was reduced after 14-3-3ζ overexpression (right panel). (**C**) In control COS-7 cells (myc–B1b/HA–B2/GFP), B1/B2 co-IP is independent of the Brefeldin A treatment (left panel). In Flag–14-3-3ζ overexpressing cells, the interaction between B1 and B2 subunits is abolished in the absence of Brefeldin A, but remains intact upon treatment with Brefeldin A (right panel). As a control, B1/B2 interaction decreases when Brefeldin A is washed out, thus allowing proteins to be properly retargeted to the plasma membrane (third band in right panel) ($n=3$ independent experiments).

Western blotting for the B2 subunit revealed that B1b/B2 association was lost at the cell membrane after 14-3-3ζ overexpression (Figure 3B). Finally, when membrane targeting of the B1/B2 dimer was prevented with Brefeldin A, the GABAB dimeric state was not altered, as monitored with co-IP in COS cells. This suggests that de-dimerization occurs only when GABAB heterodimers are targeted to the plasma membrane, thus confirming that 14-3-3ζ disrupts already formed heterodimers at the cell surface (Figure 3C).

Altogether, biochemical and biophysical approaches demonstrated that 14-3-3ζ dissociates the GABAB heterodimer. This structural modification can be blocked by disrupting B1/14-3-3ζ interaction by the mean of siRNA or competing peptides.

GABAB signalling to potassium channels is impaired by 14-3-3ζ in vitro

We investigated functional implications of 14-3-3ζ-mediated dissociation of the GABAB heterodimer. Membrane currents induced by application of Baclofen were analysed in cultures of spinal neurons using a voltage ramp and a subtraction procedure (Figure 4A1 and A2). Superfusion of Baclofen (25 μM) activated an outward current at membrane potentials near the resting potential (Figure 4A2) that became inward around the K^+ equilibrium potential (−95.8 mV) (Figure 4A1, red trace; and Figure 4A2, mean reversal potential $E_{rev}=-96.32\pm1.13$ mV). The Baclofen-induced current was blocked by CGP55845A, a specific antagonist of GABAB receptors, and usually displayed strong inward rectification

(11 out of 14 Baclofen-responsive cells tested; Supplementary Figure S7C–E), characteristic of Kir currents (Sodickson and Bean, 1996). Next, we tested the effects of 14-3-3ζ overexpression in neurons. This caused a near abolition of the Baclofen-induced potassium current, similarly to the blockade by the antagonist CGP55845A (Figure 4B, dark grey bar; $P<0.01$), without affecting the expression level of B1 and B2 (Supplementary Figure S7F). Taken together, our results showed that 14-3-3ζ-induced disruption of the heterodimer is accompanied with an inhibition of GABAB signalling *in vitro*.

Overexpressed 14-3-3ζ dissociates the GABAB receptor and impairs signalling in vivo

The consequences of 14-3-3ζ overexpression on GABAB were then tested *in vivo* in neuropathic rats. The co-detection of GABAB subunits with light microscopy showed a significant loss of B1/B2 association in neuropathic (Figure 5A and B; SNL + mmRNA versus Sham $P<0.01$) but not in Sham rats (Figure 5B). We further demonstrated that anti-14-3-3ζ siRNA intrathecal injections *in vivo* were able to restore B1/B2 colocalization in spinal neurons (Figure 5A and B; SNL + siRNA versus Sham $P>0.05$). Co-IP from spinal tissue also supported the decrease of B1/B2 association in neuropathic conditions, but not in Sham rats, and further showed that GABAB subunit interaction is restored after siRNA or competing peptide intrathecal injections (Figure 5C1). Furthermore, B1/B2 binding is inversely related to B1/14-3-3ζ association in rat models (Figure 5C2). Indeed, B1 and 14-3-3ζ were clearly associated in SNL rats while co-IP remained weak after peptide injections, and, in agreement with previous report, in sham animals (Couve *et al*, 2001). This indicated that, in normal conditions, basal levels of 14-3-3ζ interfere weakly with GABAB dimers, in contrast to overexpressed 14-3-3ζ in neuropathic conditions. We further excluded that the loss of GABAB subunits association may be due to changes in transcription (Supplementary Figure S8A) or trafficking (Supplementary Figure S8B–E).

Electron microscopy immunogold also confirmed that the close association between the GABAB subunits was disrupted in neuropathic rats whereas colocalization between endogenous B1b and 14-3-3ζ was strengthened (Figure 6). In naive and sham animals, electron microscopy immunogold confirmed tight association between B2 and B1b, both at the plasma membrane and in endoplasmic-containing domains (Figure 6Aa, d). Only few colocalizations between B1b and 14-3-3ζ were observed, mainly at the cell surface (Figure 6Ad). In SNL rats, the association between B2 and B1b was less frequent and mainly confined to the endoplasmic reticulum (Figure 6Ac). In contrast, colocalization between B1b and 14-3-3ζ was repeatedly observed at the plasma membrane (Figure 6A, c and e), although also seen within the cytoplasm (Figure 6Ae). Interestingly, the triple association of B1b, B2 and 14-3-3ζ was observed at the cell surface (Figure 6Ab).

To quantify the association between the three partners, we measured the colocalization (distance <20 nm, see Supplementary data) and the distance between particles. The percentage of B1b labelling colocalized with B2 decreased in SNL rats (Figure 6B1; $P<0.05$ SNL versus sham). In contrast, the colocalization is enhanced between B1b and 14-3-3ζ (Figure 6B1; $P<0.01$ SNL versus sham). Along with

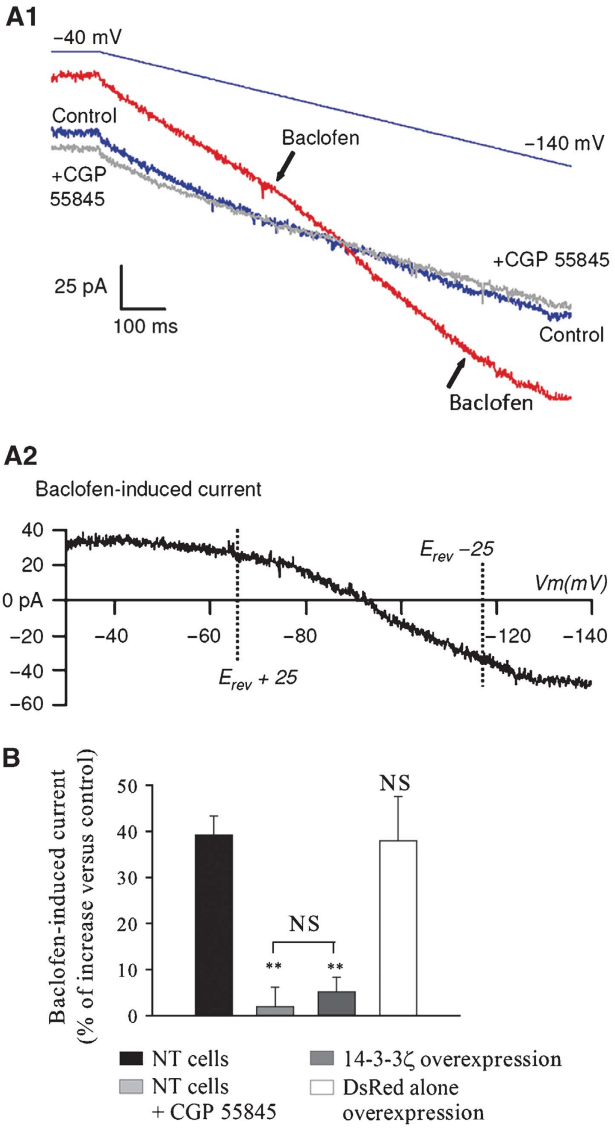

Figure 4 *In-vitro* impairment of GABAB signalling. (**A1**) Voltage ramp-evoked currents in control ACSF (blue), 25 μM Baclofen (red) and Baclofen + CGP 55845A (50 μM) (grey). (**A2**) Baclofen current resulting from the subtraction of blue plot (1) from red plot (2) as shown in Figure 3A1. (**B**) Baclofen-induced current during a voltage ramp in control (black bar, $n=13$), in the presence of 50 μM CGP 55845 (light grey bar, $P<0.01$, $n=6$), in neurons overexpressing 14-3-3ζ (dark grey bar, $P<0.01$, $n=9$), and in neurons overexpressing the DsRed vector alone (white bar, $n=8$). Results are expressed as a percentage of increase above the basal level measured in the absence of Baclofen. NT cells = non-transfected cells.

changes in colocalization rates, the distance between particles was seen as an index of their possible interaction within a single complex. The distance between B1b and B2 subunits increased significantly in SNL rats (Figure 6B2; $P<0.05$ SNL versus sham), indicating a separation between the two subunits. Conversely, the distance between B1 and 14-3-3ζ decreased in neuropathic conditions (Figure 6B2; $P<0.05$ SNL versus sham). No significant changes were observed in the relative distribution of B2 and 14-3-3ζ (Figure 6B2). No differences were noticed between naive and sham animals for any association studied.

To test for a possible alteration of GABAB signalling *in vivo*, when 14-3-3ζ is overexpressed, we performed GTP binding

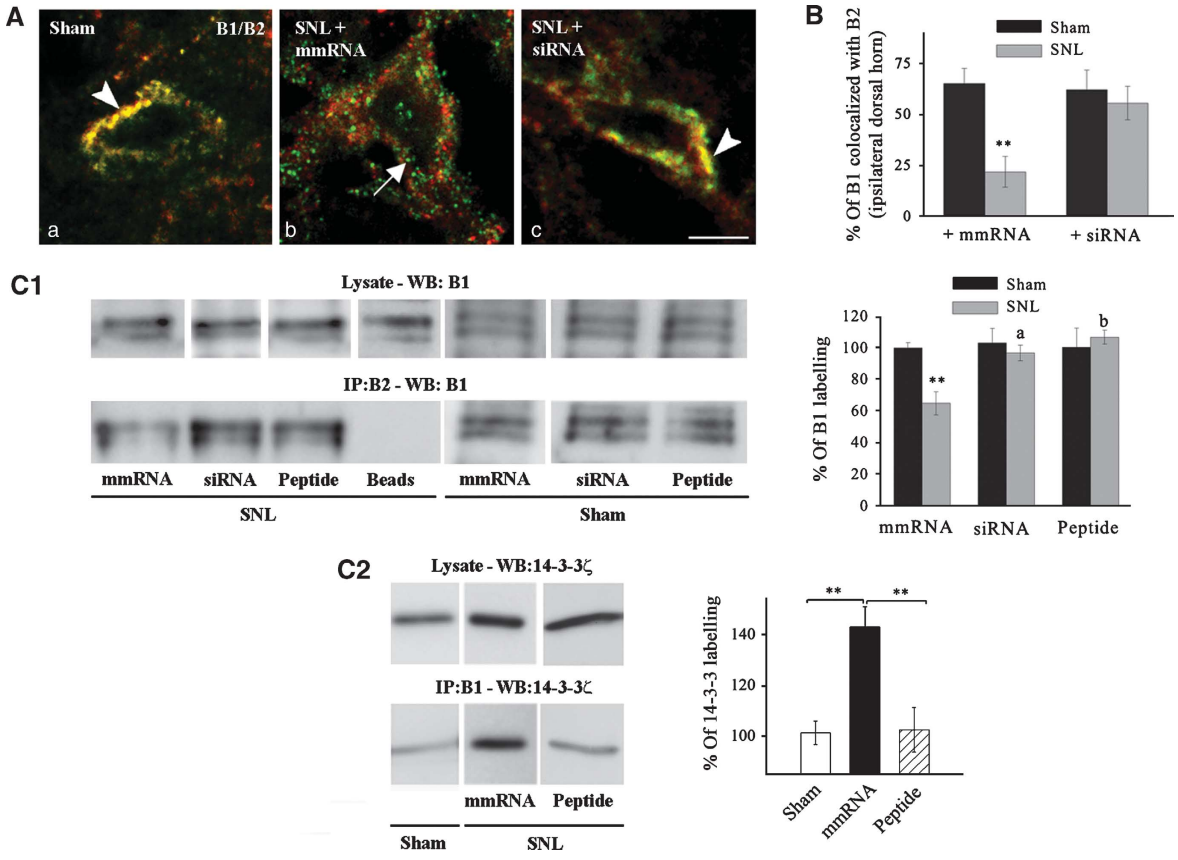

Figure 5 Decrease of endogenous co-expression of B1 and B2 in neuropathic rats. (**A**) Immunohistochemistry for endogenous B1 and B2 in lamina II of the dorsal horn of three groups of rat ($n=4$ in each group). The colocalization is prominent in sham rats (arrowhead, a). In neuropathic rats with control RNA (mmRNA) injection, B1 (green) and B2 (red) labelling were often found alone at the plasma membrane of spinal neurons (arrow, b). After siRNA injection in neuropathic rats, the colocalization is restored (arrowhead, c). Bar = 5 μm. (**B**) Quantification of the percentage of B1 colocalized with B2 labelling in lamina I–II of Sham (black bars) and SNL (grey bars) rats ($n=20$ cells in each conditions). *$P<0.05$ versus Sham. (**C1**) Co-immunoprecipitation *in vivo* showing a decrease of B1/B2 interaction in neuropathic conditions that is abolished after siRNA or competing peptide injection. No changes are detected in Sham rats upon siRNA or peptide injections. **$P<0.01$ versus Sham; a, b: $P<0.05$, $P<0.01$ versus SNL with mmRNA injection, respectively. (**C2**) Increase of B1/14-3-3ζ interaction in neuropathic conditions that is abolished after competing peptide injection. $n=5$ in each conditions. **$P<0.01$.

studies on tissue sections (Figure 7A and B, examples of autoradiograms and quantitative densitometry, respectively). In the sham group, basal [^{35}S]GTPγS binding increased both in the contralateral and ipsilateral dorsal horn after Baclofen application (131 ± 3% and 128 ± 2%, respectively). In the SNL group, Baclofen-induced increase was weaker in the ipsilateral dorsal horn (110% ± 3; $P<0.01$ versus SNL contralateral dorsal horn). In the group of SNL rats intrathecally administered with anti-14-3-3ζ siRNA, Baclofen-induced increase of [^{35}S]GTPγS binding was restored and was similar in the contralateral (130 ± 3%) and ipsilateral (131 ± 5%) dorsal horn.

In-vivo injections of 14-3-3ζ siRNAs or competing peptides partially inhibit chronic pain states

Finally, to assess the behavioural consequences of 14-3-3ζ overexpression on GABAB inhibition in chronic pain conditions, we tested the effect of disrupting 14-3-3ζ/B1 interaction on mechanical allodynia in neuropathic rats. For this purpose, we performed knock down of 14-3-3ζ by using the siRNA-based strategy or pVEC-B1 (922-930) competing peptide application, respectively. After intrathecal injections (15d), the withdrawal threshold was assessed with the von Frey test, and compared with that measured at 12 days (siRNA) or 14 days (competing peptides) after surgery. Detailed procedures are presented in Supplementary Figure S9.

SNL resulted in a decrease in paw withdrawal threshold of around 60%. The injection of vehicle after surgery did not further change the mechanical threshold of neuropathic rats (Figure 7C and E, iFect (12d) and Saline (14d), respectively). The injection of Baclofen at day 12 induced an increase in mechanical threshold indicating GABAB-mediated anti-nociceptive effects (Figure 7C, 'Baclo, 12d' versus 'iFect, 12d'; $P<0.01$). Treatments for 3 days either with control mismatched mmRNA or with anti-14-3-3ζ siRNA ('RNA, 15d') did not modify paw withdrawal thresholds which appeared similar to that observed in neuropathic rats before treatment. In contrast, the mean threshold for SNL animals after Baclofen application was significantly increased upon siRNA treatment ('RNA + Baclo, 15d' versus 'Baclo, 12d', $P<0.01$). Changes in paw withdrawal threshold were not observed in animals injected with mmRNA (black bars). The injection of anti-14-3-3ζ siRNA had no apparent side effects since it did not induce sedation in neuropathic animals (Supplementary Figure S8F; Supplementary data).

Pain behaviour was also assessed with intrathecal injections of competing peptide. Baclofen administration in neuropathic rats had anti-nociceptive effects comparable to the

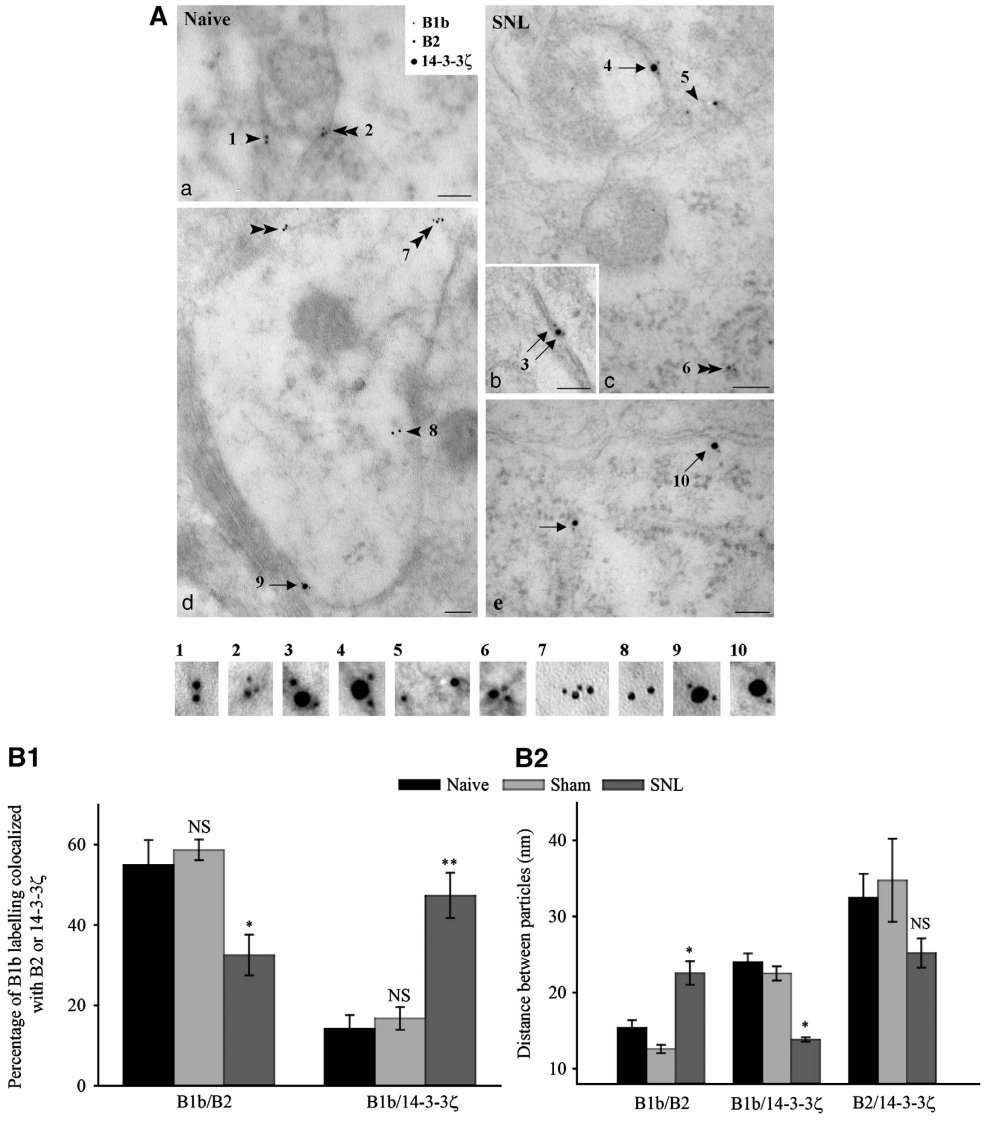

Figure 6 Changes in B1/B2 colocalization in spinal neurons at the ultrastructural level. (**A**) Triple immunogold in dorsal horn neurons of naive (a, d) and SNL (b, c, e) rats. (a, d) Isolated B2 (arrowheads) or B2 colocalization with B1b (double arrowheads). Rare association between 14-3-3ζ and B1b at the plasma membrane (arrow). (b, c and e) Prominent association between 14-3-3ζ and B1b at the plasma membrane or in the cytoplasm (arrows). Colocalization between B2 and B1b, mainly in the cytoplasm (double arrowhead). Triple colocalization showing 14-3-3ζ between B2 and B1b (double arrows). Bar: 100 nm. (**B1**) Quantification of the percentage of B1 colocalized with B2 or 14-3-3ζ (distance <20 nm). (**B2**) Quantification of distances (nm) between gold particles. Mean distances ± s.e.m. $^*P<0.05$; NS = non-significant ($n=15$ cells in each condition).

other set of experiments (Figure 7E; 'Baclo, 14d' versus 'Saline, 14d', $P<0.001$). Similarly, intrathecal injections of pVEC-B1 (922-930) together with Baclofen caused a significant increase of paw withdrawal threshold as compared with the effects of Baclofen or peptide alone (Figure 7E, 'Peptide + Baclo, 15d' versus 'Baclo, 14d' or 'Peptide, 15d'; $P<0.05$). Injection of pVEC alone did not modify mechanical threshold (Figure 7E, black bars). Interestingly, pVEC-B1 (922–930) administration in SNL animals induced *per se* a significant increase of the mean threshold as compared with neuropathic control conditions, i.e., saline injection (Figure 7E, 'Peptide, 15d' versus 'Saline, 14d', $P<0.001$). Peptide injection alone resulted in an effect that was absent with siRNA injection alone.

Our results demonstrated that disrupting 14-3-3ζ/GABAB interactions *in vivo*, with anti-14-3-3ζ siRNA or with competing peptide, specifically enhanced the anti-nociceptive effect of Baclofen on mechanical allodynia in SNL animals but had no effect in sham animals (Figure 7D and F). In addition, the present data showed that our competing peptides efficiently counteracted protein–protein interaction *in vivo*, and modified pain behaviour.

Discussion

To date, the regulation of GPCR oligomerization is known to depend on receptor targeting (McLatchie *et al*, 1998; Margeta-Mitrovic *et al*, 2000) or ligand binding (Rocheville *et al*, 2000). Our results demonstrate a novel, additional mechanism that disrupts the obligate heterodimeric state of GABAB receptors. It relies on the upregulation of 14-3-3ζ interacting protein and leads to the reduction of receptor efficacy. Importantly, this dissociation occurs in a pathophysiological context, thus contributing to disinhibition in

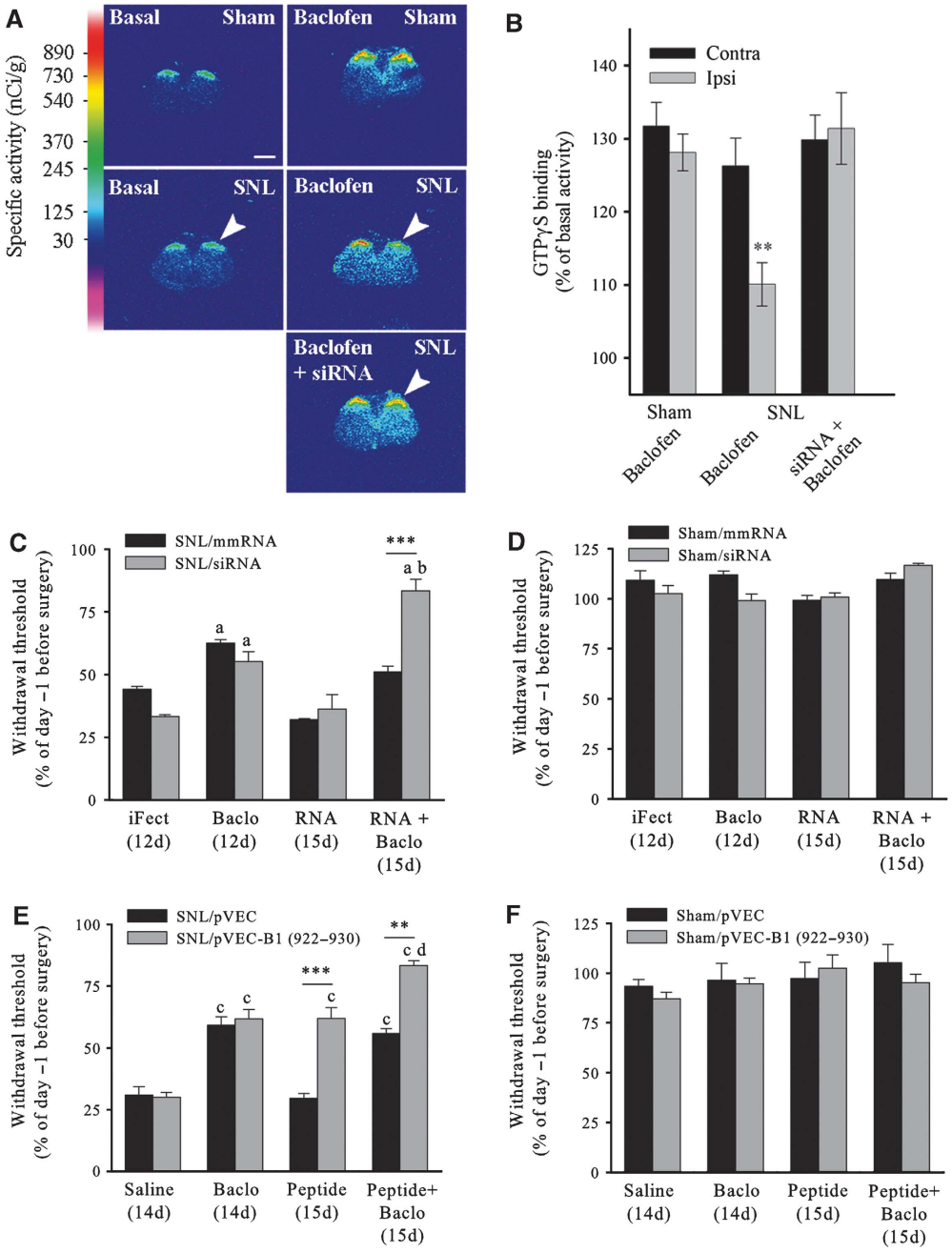

Figure 7 *In-vivo* alteration of GABAB signalling and alleviation of mechanical allodynia in SNL rats. (**A**) Autoradiographic images of [35S]GTPγS in sham and SNL rat spinal cord ($n = 5$ in each condition) showing the basal binding (left), 1 μM Baclofen-stimulated binding (right), and 1 μM Baclofen-stimulated binding after anti-14-3-3ζ siRNA injections (bottom right). Arrowheads: side ipsilateral to nerve ligation. Bar: 1.5 mm. (**B**) The quantification of GTP binding shows a decrease of GABAB activation in the ipsilateral dorsal horn of SNL rats. (**C–F**) Threshold to mechanical stimulation measured in SNL (**C**, **E**) and sham (**D**, **F**) rats before and after intrathecal injections ($n = 5$ in each condition). The threshold before surgery (day −1) is set to 100%. Baclofen produces an anti-nociceptive effect in SNL rats (**C**, Baclo, 12d; **E**, Baclo, 14d). Anti-14-3-3ζ siRNA has no effect *per se* in SNL rats (**C**, grey bars; RNA, 15d). In contrast, pVEC-B1 (922–930) has an effect similar to that of Baclofen (**E**, grey bars; peptide, 15d). The effects of Baclofen are significantly enhanced after injection of siRNA (**C**, grey bars; RNA + Baclo, 15d) or competing peptide conjugate (**E**, grey bars; peptide + Baclo, 15d). Mismatch RNA (**C**, black bars) or pVEC only (**E,** black bars) have no effect when injected alone or in conjugation with Baclofen. No changes of the mechanical threshold are seen in sham rats after intrathecal injections of Baclofen (**D, F**), siRNA (**D**, grey bars), or pVEC-B1 (922–930) (**F**, grey bars). Data are mean values ± s.e.m. $^{**}P<0.01$; $^{***}P<0.001$; a: $P<0.01$ versus iFect (12d) (**C**); b: $P<0.01$ versus SNL/siRNA, Baclo (12d) (**C**); c: $P<0.001$ versus Saline (14d) (**E**); d: $P<0.05$ versus SNL/pVEC-B1 (922–930), Baclo (14d) (**E**).

central sensitization to pain. Therefore, the present study is in line with, and further extends our previous report that chronic activation with capsaicin of an organotypic culture model induces a dissociation of the GABAB receptor, and a loss of GABAB activation (Laffray *et al*, 2007).

GABAB dimer is impaired by 14-3-3ζ interacting protein

The GABAB receptor is a class C GPCR that forms constitutive dimers. Therefore, oligomerization is necessary to the receptor functioning. In contrast, the role of oligomerization remains debated in other GPCR such as class A receptors.

In agreement with previous reports (Couve *et al*, 2001), 14-3-3ζ is shown to bind the B1 but not B2, and to compete with B2 for B1 binding. It was previously reported that 14-3-3ζ interaction may regulate receptor function (Prezeau *et al*, 1999). One identified mechanism is by promoting the dimerization of receptors and their forward trafficking to the plasma membrane (O'Kelly *et al*, 2002; Yuan *et al*, 2003). However, the situation is different for the GABAB metabotropic receptor. We showed here that 14-3-3 proteins cannot simply be viewed as scaffolding proteins in the assembly of ion channels and GPCRs, but also as regulatory proteins that impairs GPCR oligomers. Several lines of evidence support the hypothesis of GABAB de-dimerization after the heterodimer is formed. (i) There is no interaction between 14-3-3 and B1 in the endoplasmic reticulum (Brock *et al*, 2005). Moreover, we found that 14-3-3ζ is expressed at very low levels in the endoplasmic reticulum (data not shown). Therefore, 14-3-3ζ cannot simply prevent the heterodimer association. (ii) Our present data suggest that 14-3-3ζ dissociates the GABAB receptor at the plasma membrane. Moreover, B1/14-3-3ζ association is found in the vicinity of the plasma membrane with electron microscopy. Taken together, these data strongly suggest that 14-3-3ζ interacts with B1 after its insertion at the plasma membrane, or during rapid recycling of the receptor (Laffray *et al*, 2007; Grampp *et al*, 2008). Importantly, the GABAB receptor is likely to be more dynamic than other receptor in the class C sub-family since it lacks cysteine-rich domain in the extracellular part (Kniazeff *et al*, 2011). This might make the GABAB more susceptible to undergo conformational changes upon partner protein interaction. However, the possibility remains that, in addition, 14-3-3 may target B1/B2 interaction at the trans-membrane domain (Monnier *et al*, 2011) through the activation of other associated proteins.

Dissociation of the GABAB receptor weakens the transmission of nociceptive inputs

14-3-3 proteins are dimeric chaperone proteins constitutively expressed throughout the central nervous system in normal and pathological conditions (Fu *et al*, 2000; Berg *et al*, 2003). After neuronal insult, 14-3-3ζ upregulation was reported to be protective by promoting cell survival or regeneration (Murphy *et al*, 2008). Our data show that 14-3-3ζ over-expression has also detrimental effects in neuropathic pain sensitization.

Since the heterodimerization of B1 and B2 subunits is essential to the formation of a functional class C receptor (Margeta-Mitrovic *et al*, 2000), dimer alteration is expected to cause a loss of function of the GABAB receptor. Indeed, we show here that GABAB signalling to the G-protein cascade (*in vivo*), and coupling to cellular effectors such as Kir channels, were altered by 14-3-3ζ overexpression (*in vitro*). Moreover, the local knockdown of 14-3-3ζ restores GABAB signalling in superficial laminae of neuropathic rats and enhances the efficiency of exogenously applied Baclofen to attenuate spinal sensitization, showing the importance of de-dimerization mechanisms in pathophysiological processes *in vivo*. Finally, GABAB impairment could explain how neuropathic conditions triggered the expression of calcium-dependent plateau potentials (Reali *et al*, 2011) that are normally inhibited by GABAB activation (Derjean *et al*, 2003). These results are in agreement with the loss of GABAB agonist binding in the spinal cord of pain models (Castro-Lopes *et al*, 1995).

In-vivo co-IP and histological analysis confirmed the interaction between B1 and 14-3-3ζ and the loss of B1/B2 association in spinal neurons of neuropathic rats. The dissociation may be a pivotal mechanism that limits GABAB activation in neuropathic conditions. It may act jointly with other mechanisms, e.g., possible downregulation of GABAB subunits (Wu *et al*, 2011). GABAB is de-dimerized, and signalling is impaired essentially when 14-3-3ζ is overexpressed. Such condition occurs not only *in vitro* upon neuronal transfection, but also naturally *in vivo* in neuropathic rats. In contrast, in sham animals, interaction between B1 and 14-3-3ζ remains weak and knockdown of 14-3-3ζ did not modify mechanical sensitivity in these animals. In neuropathic rats, 14-3-3ζ was detected in presynaptic and postsynaptic compartments. Therefore, the interaction is likely to occur in both compartments, thus affecting B2/B1a and B2/B1b heterodimers.

Overexpression of 14-3-3ζ leads only to partial dissociation of the B1/B2 heterodimer, as shown here with 2P-FLIM. In addition, although largely reduced, the GABAB receptor retains some capacity to activate G-protein coupling. However, GABAB-mediated opening of Kir channels is fully impaired in neuronal cultures. We conclude that below a certain threshold level, remaining heterodimeric GABAB receptors are not sufficient to drive strong enough activation of intracellular targets, and to inhibit pain sensitization. 14-3-3ζ silencing restores a level of functional heterodimers that permits GABAB inhibition to reduce allodynia.

Clinical perspectives

We detected 14-3-3ζ upregulation in SNL rat dorsal horn, but not in the ventral horn. Moreover, the analysis of locomotor activity indicates that 14-3-3ζ overexpression in the dorsal horn does not affect motor control in the ventral horn. These data are in line with the actual recommendations for clinical use of Baclofen. In fact, Baclofen administration is not proposed in EFNS guidelines of pharmacological treatment of neuropathic pain and its general effectiveness as an analgesic is limited (Attal *et al*, 2006). In contrast, intrathecal Baclofen offers one of the best options in many patients with severe spasticity (Hsieh and Penn, 2006) because of its action on spinal motoneurons (Bowery *et al*, 2002). Taken together, these data further confirm that GABAB is impaired only where 14-3-3ζ is overexpressed and weakens inhibitory signalling, i.e., in the dorsal but not in the ventral horn. Therefore, our results suggest that co-application of 14-3-3ζ inhibitor could enhance Baclofen effect to alleviate neuropathic pain in clinic.

In conclusion, our results provide new insights in cell biology of GPCRs. We reveal a novel mechanism that impairs GPCR activity based on interactions with a chaperone protein. Together with other mechanisms involving modulation of inhibitory transmission (Moore *et al*, 2002; Bardoni *et al*, 2007; Ferrini *et al*, 2010), or loss of GABAA inhibition (Coull *et al*, 2005; Knabl *et al*, 2008), our data support the view that disinhibition dramatically twists the excitability of spinal neurons and leads to pain sensitization (Woolf and Salter, 2000). Targeting the GABAB dissociation process may

be of therapeutic interest by enhancing the action of classical pain killers.

Materials and methods

Cell cultures and transfection

Dissociated rat spinal neurons, or COS-7 cells were transiently transfected with various constructs or siRNA using the procedures described in Supplementary data.

Immunohistochemistry on spinal cell cultures

Immunodetection in cell cultures was carried out sequentially according to previously published protocols as detailed in Supplementary data.

Colocalization of myc–B1b with HA–B2 or Flag–14-3-3ζ, or colocalization of HA–B2 with Flag–14-3-3ζ was quantified as the percentage of colocalized area of the total labelled area in double and triple transfected cells. We also measured staining intensity correlation (see Supplementary data). This method discriminates colocalization between interacting proteins, whose staining intensity should vary in synchrony from randomly colocalized proteins, whose overlapping might be due to the broad distribution of one protein across the cell.

qRT–PCR

Expression analysis of 14-3-3ζ, 14-3-3η, B1 and B2 mRNA was performed with the DyNAmo^{TM} SYBR Green qPCR kit (Finnzymes, Espoo, Finland). Triplicate runs were performed and Succinate dehydrogenase Complex, Subunit A (SDHA) was used as a normalizer. The relative level of expression was calculated using the comparative ($2^{\Delta\Delta CT}$) method.

Immunoprecipitation

Co-IP was performed after transfection in COS-7 cells as described in Supplementary data. Total proteins, immunoprecipitated proteins and supernatant proteins were loaded into L, IP and S lanes, respectively. Proteins were then transferred, probed with anti-Flag, anti-myc or anti-HA antibodies (1/1000), and visualized with enhanced chemiluminescence.

In vivo, protein extraction was performed according to a similar protocol, adapted from Benke *et al* (1999). Antibodies used for immunoprecipitation were anti-GABAB2 from BD Biosciences, and anti GABAB1 from Abcam (ab 55051). Western blot detection used anti-14-3-3ζ (Santa Cruz Biotechnology), and anti-GABAB1 (gift from Dr Gassmann).

The density of bands was quantitated by densitometry using a Syngene machine (ChemiGenius 2XE model; Synoptics Ltd, Cambridge, UK) and Genetool analysis programme (Syngene). For immunoprecipitation, immunoblots were semiquantified by normalizing the IP band density to that of the lysate band.

Competing peptides

Two different competing peptides were used, corresponding to amino acids 919–927 or 922–930 of the GABAB1 protein. Peptides sequences were used as native sequences, or modified by adding positively charged amino acids, or by coupling to the cell penetrating peptide pVEC, derived from the cell adhesion molecule vascular endothelial cadherin (Elmquist *et al*, 2001). Competing peptides and pVEC were synthesized with Fmoc and t-Boc methods, respectively, purified, and then conjugated (see Supplementary data). For some experiments, peptides were labelled with carboxyfluorescein (see all sequences used in Supplementary Figure S5). For *in-vitro* experiments, cells were treated for 1 h with 1 μM peptide solution, washed and detached (COS-7 cells) or fixed (primary cultures). No differences were seen when using 5 μM peptide solution (data not shown).

Peptide and conjugate uptake was studied with confocal microscopy after incubating 1 μM peptide solutions for 1 h at 4 and 37°C, or after inhibiting endocytosis with Wortmanin. Fluoresceinyl-peptide uptake was further quantified by fluorometry. Cytotoxicity was assessed with Lactate Dehydrogenase assay.

Spectral and lifetime correlated acquisitions

The interaction between GFP-tagged proteins and t-dimer DsRed-tagged proteins was studied using quantitative FRET determination with FLIM using Time Correlated-Single Photon Counting (Becker and Hickl, Berlin, Germany) as detailed in Supplementary data.

To assess protein interactions, we calculated a relative FRET efficiency for each acquisition as: FRET efficiency (%) = $(\tau_{Dmean} - \tau_{DA})/\tau_{Dmean} \times 100$ where τ is the time constant of the exponential fit with τ_{Dmean} being the mean lifetime of the donor fluorophore (GFP) when expressed alone and τ_{DA} being the lifetime of the donor fluorophore in the presence of the acceptor (t-dimer DsRed). Results were expressed as a mean FRET efficiency ($n = 31$ or 21 cells in each condition) ± s.e.m.

Patch clamp

Experiments were conducted as previously described (Derjean *et al*, 2003). Voltage-clamp recordings were performed on 8- to 10-day-aged cultured spinal neurons. The following drugs were added to the normal Krebs solution and continuously superfused on the preparation: 25 μM Baclofen (Sigma), 50 μM CGP55845 (Fisher Bioblock Scientific, Illkirch, France). Cs^+ was added to a modified perfusion medium. The detailed experimental set-up and data analysis procedure are described in Supplementary data.

Animal models and behavioural tests

A total number of 136 adult male Wistar rats (250–300 g; Charles River France, St Aubin les Elbeuf, France) were used. The experiments followed the ethical guidelines of the International Association for the Study of Pain and were approved by the local ethics committee in Bordeaux (AP 1/04/2005).

Persistent neuropathic pain in rats was evoked with SNL (Kim and Chung, 1992). Mechanical response thresholds were monitored with the von Frey test as described in Supplementary data.

Western blotting

Briefly, tissue homogenates from lumbar spinal cord segments of sham or SNL animals were loaded onto SDS–PAGE, transferred, probed with appropriate antibodies, detected with enhanced chemiluminescence (Amersham Biosciences, Buckinghamshire, UK) and visualized with a Syngene system (Synoptics Ltd). Tubulin or GAPDH was used as loading control.

In-situ hybridization

Cryostat sections from SNL, sham-operated and naive animals ($n = 5$ in each group) were hybridized with three different oligonucleotide probes complementary to 14-3-3ζ mRNA. The procedures for *in-situ* hybridization and quantification are described in Supplementary data.

Immunohistochemistry on tissue sections

Naive, sham and various groups of SNL-operated animals (+ iFect, + siRNA, + peptides) were processed for immunohistochemistry with light ($n = 5$ in each group) and electron ($n = 3$ in each group) microscopy, after intracardiac perfusion. Labelling intensity or surface colocalization was measured with Metamorph software. For electron microscopy, tissue samples from deep dorsal horn laminae were processed for post-embedding immunogold labelling (see Supplementary data). The colocalization and distance between gold particle pairs were measured on digitalized micrographs with Image J software. Results were expressed as the mean colocalization or distance (nm) between pairs ± s.e.m. The detailed procedures and antibodies are described in Supplementary data.

GTPγS binding

The [35S]GTPγS) binding autoradiographic procedure was carried out as described in Supplementary data. [35S]GTPγS binding was measured in transverse lumbar spinal cord sections from sham, and SNL animals, and SNL with siRNA injections ($n = 5$ in each condition).

In-vivo intrathecal injections and behavioural tests

For intrathecal injections of Baclofen, RNAs (anti-14-3-3ζ siRNA or mismatch RNA), or peptide conjugates (pVEC-B1 (922–930) or pVEC alone), sham and SNL rats were implanted with a catheter. The threshold to mechanical stimulation was monitored before and after surgery, and after the various injections. Results were expressed as percentages of changes in the threshold of neuropathic rats.

The open field method was used to evaluate spontaneous horizontal locomotor activity of sham or neuropathic rats after i-Fect or anti-14-3-3ζ siRNA injections.

The experimental schedules are presented in Supplementary Figure S9, and the detailed procedures are described in Supplementary data.

Statistical analysis

Student's *t*-tests were used to compare two series of data. Kruskal–Wallis one-way Analyses of Variance (ANOVAs) coupled with Dunn's *post hoc* comparison was used to analyse non-parametric sets of data. One-way or two-way ANOVAs were performed for parametric data analyses, associated with Newman–Keuls tests for *post hoc* comparisons. $P<0.05$ was considered significant.

Supplementary data

Supplementary data are available at *The EMBO Journal* Online (http://www.embojournal.org).

Acknowledgements

This study was supported by the 'Conseil Régional d'Aquitaine' (#2008/30/023), the ANR (ANR-07-neuro-015-01), and the 'Fondation de France' (#RAF05020GGA). U Langel is grateful to the Swedish Research Council (VR-NT and VR-Med). We are grateful to Dr R Tsien (Department of Pharmacology, UCSD, CA) and to Dr H Fu (Department of Pharmacology, Emory University, GA) for the generous gifts of the t-dimer DsRed pRSET B and Flag–14-3-3ζ/histidine-14-3-3η pcDNA3 constructs, respectively. We thank Dr A Calver (GlaxoSmithKline Pharmaceuticals, UK) and Dr JP Pin (IGF, Montpellier, France) for the gift of myc–B1b and HA–B2 pcDNA3, and of $B1_{ASA}$-GFP pcDNA plasmids, respectively. We thank Dr M Gassmann (Department of Biomedicine, University of Basel, Switzerland) for the generous gift of the anti-GABAB1 antibody used in western blot. We thank Dr C Poujol and P Legros (BIC, Bordeaux University) for help in FRET imaging. We thank Dr C Baudet and P Rottiers for help in co-immunoprecipitation experiments.

Author contributions: SL and ML wrote the manuscript, conceived the experiments, performed the experiments, and analysed the data. RBB, MAP and AF performed the experiments and analysed the data. YJ, TH, CS, PF, YLF and MD performed the experiments. PD and LH conceived the experiments and analysed the data. UL conceived the experiments. FN wrote the manuscript, conceived the experiments and analysed the data.

Conflict of interest

The authors declare that they have no conflict of interest.

References

Attal N, Cruccu G, Haanpaa M, Hansson P, Jensen TS, Nurmikko T, Sampaio C, Sindrup S, Wiffen P (2006) EFNS guidelines on pharmacological treatment of neuropathic pain. *Eur J Neurol* **13:** 1153–1169

Bardoni R, Ghirri A, Salio C, Prandini M, Merighi A (2007) BDNF-mediated modulation of GABA and glycine release in dorsal horn lamina II from postnatal rats. *Dev Neurobiol* **67:** 960–975

Benke D, Honer M, Michel C, Bettler B, Mohler H (1999) gamma-aminobutyric acid type B receptor splice variant proteins GBR1a and GBR1b are both associated with GBR2 *in situ* and display differential regional and subcellular distribution. *J Biol Chem* **274:** 27323–27330

Berg D, Holzmann C, Riess O (2003) 14-3-3 proteins in the nervous system. *Nat Rev Neurosci* **4:** 752–762

Bouvier M (2001) Oligomerization of G-protein-coupled transmitter receptors. *Nat Rev Neurosci* **2:** 274–286

Bowery NG (2006) GABAB receptor: a site of therapeutic benefit. *Curr Opin Pharmacol* **6:** 37–43

Bowery NG, Bettler B, Froestl W, Gallagher JP, Marshall F, Raiteri M, Bonner TI, Enna SJ (2002) International Union of Pharmacology. XXXIII. Mammalian gamma-aminobutyric acid(B) receptors: structure and function. *Pharmacol Rev* **54:** 247–264

Brock C, Boudier L, Maurel D, Blahos J, Pin JP (2005) Assembly-dependent surface targeting of the heterodimeric GABAB receptor is controlled by COPI but not 14-3-3. *Mol Biol Cell* **16:** 5572–5578

Castro-Lopes JM, Malcangio M, Pan BH, Bowery NG (1995) Complex changes of GABAA and GABAB receptor binding in the spinal cord dorsal horn following peripheral inflammation or neurectomy. *Brain Res* **679:** 289–297

Comps-Agrar L, Kniazeff J, Norskov-Lauritsen L, Maurel D, Gassmann M, Gregor N, Prezeau L, Bettler B, Durroux T, Trinquet E, Pin JP (2011) The oligomeric state sets GABA(B) receptor signalling efficacy. *EMBO J* **30:** 2336–2349

Coull JA, Beggs S, Boudreau D, Boivin D, Tsuda M, Inoue K, Gravel C, Salter MW, De Koninck Y (2005) BDNF from microglia causes the shift in neuronal anion gradient underlying neuropathic pain. *Nature* **438:** 1017–1021

Couve A, Kittler JT, Uren JM, Calver AR, Pangalos MN, Walsh FS, Moss SJ (2001) Association of GABA(B) receptors and members of the 14-3-3 family of signaling proteins. *Mol Cell Neurosci* **17:** 317–328

Derjean D, Bertrand S, Le Masson G, Landry M, Morisset V, Nagy F (2003) Dynamic balance of metabotropic inputs causes dorsal horn neurons to switch functional states. *Nat Neurosci* **6:** 274–281

Elmquist A, Lindgren M, Bartfai T, Langel U (2001) VE-cadherin-derived cell-penetrating peptide, pVEC, with carrier functions. *Exp Cell Res* **269:** 237–244

Fairfax BP, Pitcher JA, Scott MG, Calver AR, Pangalos MN, Moss SJ, Couve A (2004) Phosphorylation and chronic agonist treatment atypically modulate GABAB receptor cell surface stability. *J Biol Chem* **279:** 12565–12573

Ferrini F, Salio C, Lossi L, Gambino G, Merighi A (2010) Modulation of inhibitory neurotransmission by the vanilloid receptor type 1 (TRPV1) in organotypically cultured mouse substantia gelatinosa neurons. *Pain* **150:** 128–140

Franek M, Vaculin S, Rokyta R (2004) GABA(B) receptor agonist baclofen has non-specific antinociceptive effect in the model of peripheral neuropathy in the rat. *Physiol Res* **53:** 351–355

Fu H, Subramanian RR, Masters SC (2000) 14-3-3 proteins: structure, function, and regulation. *Annu Rev Pharmacol Toxicol* **40:** 617–647

Galvez T, Duthey B, Kniazeff J, Blahos J, Rovelli G, Bettler B, Prezeau L, Pin JP (2001) Allosteric interactions between GB1 and GB2 subunits are required for optimal GABA(B) receptor function. *EMBO J* **20:** 2152–2159

Gonzalez-Maeso J, Ang RL, Yuen T, Chan P, Weisstaub NV, Lopez-Gimenez JF, Zhou M, Okawa Y, Callado LF, Milligan G, Gingrich JA, Filizola M, Meana JJ, Sealfon SC (2008) Identification of a serotonin/glutamate receptor complex implicated in psychosis. *Nature* **452:** 93–97

Grampp T, Notz V, Broll I, Fischer N, Benke D (2008) Constitutive, agonist-accelerated, recycling and lysosomal degradation of GABA(B) receptors in cortical neurons. *Mol Cell Neurosci* **39:** 628–637

Gurevich VV, Gurevich EV (2008) GPCR monomers and oligomers: it takes all kinds. *Trends Neurosci* **31:** 74–81

Holman D, Henley JM (2007) A novel method for monitoring the cell surface expression of heteromeric protein complexes in dispersed neurons and acute hippocampal slices. *J Neurosci Methods* **160:** 302–308

Hsieh JC, Penn RD (2006) Intrathecal baclofen in the treatment of adult spasticity. *Neurosurg Focus* **21:** e5

Jones KA, Borowsky B, Tamm JA, Craig DA, Durkin MM, Dai M, Yao WJ, Johnson M, Gunwaldsen C, Huang LY, Tang C, Shen Q, Salon JA, Morse K, Laz T, Smith KE, Nagarathnam D, Noble SA, Branchek TA, Gerald C (1998) GABA(B) receptors function as a heteromeric assembly of the subunits GABA(B)R1 and GABA(B)R2. *Nature* **396:** 674–679

Kaupmann K, Malitschek B, Schuler V, Heid J, Froestl W, Beck P, Mosbacher J, Bischoff S, Kulik A, Shigemoto R, Karschin A, Bettler B (1998) GABA(B)-receptor subtypes assemble into functional heteromeric complexes. *Nature* **396:** 683–687

Kim SH, Chung JM (1992) An experimental model for peripheral neuropathy produced by segmental spinal nerve ligation in the rat. *Pain* **50:** 355–363

Knabl J, Witschi R, Hosl K, Reinold H, Zeilhofer UB, Ahmadi S, Brockhaus J, Sergejeva M, Hess A, Brune K, Fritschy JM, Rudolph U, Mohler H, Zeilhofer HU (2008) Reversal of pathological pain through specific spinal GABAA receptor subtypes. *Nature* **451:** 330–334

Kniazeff J, Prezeau L, Rondard P, Pin JP, Goudet C (2011) Dimers and beyond: The functional puzzles of class C GPCRs. *Pharmacol Ther* **130:** 9–25

Laffray S, Tan K, Dulluc J, Bouali-Benazzouz R, Calver AR, Nagy F, Landry M (2007) Dissociation and trafficking of rat $GABA_B$ receptor heterodimer upon capsaicin treatment. *Eur J Neurosci* **25:** 1402–1416

Lagerstrom MC, Schioth HB (2008) Structural diversity of G protein-coupled receptors and significance for drug discovery. *Nat Rev Drug Discov* **7:** 339–357

Loubser PG, Akman NM (1996) Effects of intrathecal baclofen on chronic spinal cord injury pain. *J Pain Symptom Manage* **12:** 241–247

Malcangio M, Bowery NG (1996) GABA and its receptors in the spinal cord. *Trends Pharmacol Sci* **17:** 457–462

Margeta-Mitrovic M, Jan YN, Jan LY (2000) A trafficking checkpoint controls GABA(B) receptor heterodimerization. *Neuron* **27:** 97–106

McLatchie LM, Fraser NJ, Main MJ, Wise A, Brown J, Thompson N, Solari R, Lee MG, Foord SM (1998) RAMPs regulate the transport and ligand specificity of the calcitonin-receptor-like receptor. *Nature* **393:** 333–339

Monnier C, Tu H, Bourrier E, Vol C, Lamarque L, Trinquet E, Pin JP, Rondard P (2011) Trans-activation between 7TM domains: implication in heterodimeric GABA(B) receptor activation. *EMBO J* **30:** 32–42

Moore KA, Kohno T, Karchewski LA, Scholz J, Baba H, Woolf CJ (2002) Partial peripheral nerve injury promotes a selective loss of GABAergic inhibition in the superficial dorsal horn of the spinal cord. *J Neurosci* **22:** 6724–6731

Murphy N, Bonner HP, Ward MW, Murphy BM, Prehn JH, Henshall DC (2008) Depletion of 14-3-3 zeta elicits endoplasmic reticulum stress and cell death, and increases vulnerability to kainate-induced injury in mouse hippocampal cultures. *J Neurochem* **106:** 978–988

O'Kelly I, Butler MH, Zilberberg N, Goldstein SA (2002) Forward transport. 14-3-3 binding overcomes retention in endoplasmic reticulum by dibasic signals. *Cell* **111:** 577–588

Panetta R, Greenwood MT (2008) Physiological relevance of GPCR oligomerization and its impact on drug discovery. *Drug Discov Today* **13:** 1059–1066

Perroy J, Adam L, Qanbar R, Chenier S, Bouvier M (2003) Phosphorylation-independent desensitization of GABA(B) receptor by GRK4. *EMBO J* **22:** 3816–3824

Pozuelo Rubio M, Geraghty KM, Wong BH, Wood NT, Campbell DG, Morrice N, Mackintosh C (2004) 14-3-3-affinity purification of over 200 human phosphoproteins reveals new links to regulation of cellular metabolism, proliferation and trafficking. *Biochem J* **379:** 395–408

Prezeau L, Richman JG, Edwards SW, Limbird LE (1999) The zeta isoform of 14-3-3 proteins interacts with the third intracellular loop of different alpha2-adrenergic receptor subtypes. *J Biol Chem* **274:** 13462–13469

Reali C, Fossat P, Landry M, Russo RE, Nagy F (2011) Intrinsic membrane properties of spinal dorsal horn neurones modulate nociceptive information processing *in vivo*. *J Physiol* **589:** 2733–2743

Rocheville M, Lange DC, Kumar U, Sasi R, Patel RC, Patel YC (2000) Subtypes of the somatostatin receptor assemble as functional homo- and heterodimers. *J Biol Chem* **275:** 7862–7869

Schuler V, Luscher C, Blanchet C, Klix N, Sansig G, Klebs K, Schmutz M, Heid J, Gentry C, Urban L, Fox A, Spooren W, Jaton AL, Vigouret J, Pozza M, Kelly PH, Mosbacher J, Froestl W, Kaslin E, Korn R *et al* (2001) Epilepsy, hyperalgesia, impaired memory, and loss of pre- and postsynaptic GABA(B) responses in mice lacking GABA(B(1)). *Neuron* **31:** 47–58

Schwenk J, Metz M, Zolles G, Turecek R, Fritzius T, Bildl W, Tarusawa E, Kulik A, Unger A, Ivankova K, Seddik R, Tiao JY, Rajalu M, Trojanova J, Rohde V, Gassmann M, Schulte U, Fakler B, Bettler B (2010) Native GABA(B) receptors are heteromultimers with a family of auxiliary subunits. *Nature* **465:** 231–235

Sodickson DL, Bean BP (1996) GABAB receptor-activated inwardly rectifying potassium current in dissociated hippocampal CA3 neurons. *J Neurosci* **16:** 6374–6385

Szidonya L, Cserzo M, Hunyady L (2008) Dimerization and oligomerization of G-protein-coupled receptors: debated structures with established and emerging functions. *J Endocrinol* **196:** 435–453

Vargas KJ, Terunuma M, Tello JA, Pangalos MN, Moss SJ, Couve A (2008) The availability of surface GABA B receptors is independent of gamma-aminobutyric acid but controlled by glutamate in central neurons. *J Biol Chem* **283:** 24641–24648

Vigot R, Barbieri S, Brauner-Osborne H, Turecek R, Shigemoto R, Zhang YP, Lujan R, Jacobson LH, Biermann B, Fritschy JM, Vacher CM, Muller M, Sansig G, Guetg N, Cryan JF, Kaupmann K, Gassmann M, Oertner TG, Bettler B (2006) Differential compartmentalization and distinct functions of GABAB receptor variants. *Neuron* **50:** 589–601

Wang XL, Zhang HM, Chen SR, Pan HL (2007) Altered synaptic input and GABAB receptor function in spinal superficial dorsal horn neurons in rats with diabetic neuropathy. *J Physiol* **579:** 849–861

Woolf CJ, Salter MW (2000) Neuronal plasticity: increasing the gain in pain. *Science* **288:** 1765–1769

Wu J, Xu Y, Pu S, Jiang W, Du D (2011) p38/MAPK inhibitor modulates the expression of dorsal horn GABA(B) receptors in the spinal nerve ligation model of neuropathic pain. *Neuroimmunomodulation* **18:** 150–155

Yuan H, Michelsen K, Schwappach B (2003) 14-3-3 dimers probe the assembly status of multimeric membrane proteins. *Curr Biol* **13:** 638–646